Accelerator Division
Alternating Gradient Synchrotron Department
BROOKHAVEN NATIONAL LABORATORY
Upton, New York 11973

Accelerator Division
Technical Note

AGS/AD/Tech. Note No. 375

BUNCHED BEAM LONGITUDINAL INSTABILITY--

COHERENT DIPOLE MOTION

S.Y. Zhang and W.T. Weng

April 15, 1993

BUNCHED BEAM LONGITUDINAL INSTABILITY - COHERENT DIPOLE MOTION

S.Y. Zhang and W.T. Weng

AGS Department, Brookhaven National Laboratory,
Upton, New York 11973

ABSTRACT

In this paper, we present a new formulation for the longitudinal coherent dipole motion, where a quadrature response of the environmental impedance is shown to be the effective longitudinal impedance for the beam instability. The Robinson-Pedersen formulation for the longitudinal dipole motion is also presented, the difference of the two approaches is discussed in the comparison. The results by using the Sacherer integral equation for the coherent dipole motion can generate the same results as by using the other two approaches, except for a scaling difference. The formulation is further generalized to the rigid bunch motion using signal analysis method, where a form factor shows up naturally. Finally, the formulation is applied to solve the coupled bunch instabilities. Examples of the AGS Booster and the AGS coupled bunch instabilities are used to illustrate the applications of the formulation.

I. Introduction

In this paper, we present a new formulation for the longitudinal coherent dipole motion. The formulation is based on the idealized condition of the synchrotron oscillation modulated by the RF frequency. We will show that for the longitudinal coherent motion, the quadrature response of the environmental impedance to the beam signal represents an effective longitudinal impedance. The Robinson-Pedersen approach to the same problem is also presented, and the comparison shows the difference of the two approaches, the results however are the identical. In Sacherer integral equation, the Vlasov equation is used to consider the particle density evolution in the phase space, the results of the coherent dipole instabilities are shown to be different by a scaling factor from other two approaches.

By considering the rigid bunch beam signal and the associated impedance, the formulation will be further generalized to the rigid bunch motion. A form factor under this condition will be developed. Finally, the coupled bunch instability is studied as a special case of the longitudinal coherent motion, and the application of the presented formulation gives rise to several results. Two examples at the AGS Booster and the AGS will be presented to illustrate the application of the formulation.

II. The New Formulation

In this section, we present a formulation for the bunched beam coherent dipole motion. In the longitudinal motion, the beam performs a synchrotron oscillation. This oscillation is modulated by the RF carrier. The induced voltage through the longitudinal impedance, for instance the RF cavities, may affect the synchrotron oscillation and cause the beam instability. A model of the beam dynamics based on the longitudinal impedance will be proposed. It will be shown that under the RF frequency modulation and demodulation, a quadrature response of the longitudinal impedance with respect to the RF carrier will be the dominant impedance and therefore to contribute to the beam instability.

2.1. Beam Dynamic Model

In Fig.1, a dipole motion model is shown, where each block represents a transfer function between two variables, and s is the Laplace operator. ω_O and ω_{RF} are the revolution and RF frequencies, respectively. Let h be the harmonic number, we have $\omega_{RF} = h\,\omega_O$. β is the ratio of the particle velocity and the light velocity, and E is the total energy of the particle. Throughout this paper, only the situation below transition is considered, therefore the frequency slip factor η is negative. V and ϕ_S are the RF voltage amplitude and the synchronous phase, respectively. We use ϕ, ΔE and ΔV to denote the phase, energy and the equivalent voltage deviations from the equilibrium state. ΔV_B is the equivalent RF gap voltage deviation caused by the beam motion itself, and ΔV_{CAV} caused by the cavity voltage variation. I_B is the beam current amplitude of the fundamental frequency, i.e., the RF frequency. Finally, $Z_M(s)$ represents the longitudinal impedance, where the subscript M denotes that the impedance is not a conventional one but under the consideration of RF modulation and demodulation.

In the block diagram, the upper loop represents the synchrotron oscillation, where the following relations are used [15],

$$\Delta E = \frac{e\,\omega_O\,V\cos\phi_S}{2\pi s}\,\phi \tag{2-1}$$

and

$$\phi = \frac{\omega_{RF}\,\eta}{\beta^2 E s}\,\Delta E \tag{2-2}$$

Since we have

$$\Delta E = \frac{e\,\omega_O}{2\pi s}\,\Delta V \tag{2-3}$$

it follows,

$$\Delta V_B = V\cos\phi_S\;\phi \tag{2-4}$$

which indicates that under the linearization, if $\phi_S = 0$, then 1 *rad* of beam phase deviation will be equivalent to the RF cavity voltage variation with full RF voltage amplitude V.

The lower loop represents the effects of the beam current to the cavity voltage through the longitudinal impedance. Note that under the linearization the transmission relation between ϕ and the beam current variation ΔI_B is I_B. Now what remains to solve is the impedance $Z_M(s)$.

2.2. Impedance

In the beam dynamic diagram represented by the transfer functions, e.g., in Fig.1, the Laplace transform is used. To discuss the impedance where the modulation and demodulation are involved, the Fourier transform is convenient. In this article, both transforms will be used. For instance, an impedance in the Laplace form can be $Z(s+j\omega_{RF})$, and its counterpart in the Fourier form is written as $Z(\omega+\omega_{RF})$, where we used $s=j\omega$.

In this section, we will show that the impedance $Z_M(s)$ in Fig.1 is,

$$Z_M(s) = \frac{1}{2j}\left(Z(s+j\omega_{RF}) - Z(s-j\omega_{RF}) \right) \tag{2-5}$$

Consider a general situation of modulated input and output. Let the input signal of a system be $f(t)$ and the output be $g(t)$. The input signal is assumed to be a low frequency signal $f_L(t)$ modulated by an RF frequency, say $\cos\omega_{RF}t$, i.e., we can write,

$$f(t) = f_L(t)\cos\omega_{RF}t \tag{2-6}$$

If we use $f(t) \rightarrow F(\omega)$ and $f_L(t) \rightarrow F_L(\omega)$ to denote the Fourier pairs, then we have,

$$F(\omega) = \frac{1}{2}\left(F_L(\omega+\omega_{RF}) + F_L(\omega-\omega_{RF}) \right) \tag{2-7}$$

Also if,

$$f_1(t) = f_L(t)\sin\omega_{RF}t \tag{2-8}$$

then we have,

$$F_1(\omega) = \frac{1}{2j}\left(F_L(\omega+\omega_{RF}) - F_L(\omega-\omega_{RF}) \right) \tag{2-9}$$

Under the modulation of the frequency ω_{RF}, the in-phase and quadrature responses due to the impedance $Z(\omega)$ with respect to the RF carrier are defined by [8],

$$Z_P(\omega) = \frac{1}{2}\,(\,Z(\omega+\omega_{RF}) + Z(\omega-\omega_{RF})\,) \tag{2-10}$$

and

$$Z_Q(\omega) = \frac{1}{2j}\,(\,Z(\omega+\omega_{RF}) - Z(\omega-\omega_{RF})\,) \tag{2-11}$$

respectively. We also define

$$G_P(\omega) = F_L(\omega)Z_P(\omega) \tag{2-12}$$

and

$$G_Q(\omega) = F_L(\omega)Z_Q(\omega) \tag{2-13}$$

If the Fourier pairs $g_P(t) \rightarrow G_P(\omega)$ and $g_Q(t) \rightarrow G_Q(\omega)$ are used, the total response through the impedance $Z(\omega)$ for the modulated signal $F(\omega)$ in (2-7) can be written as,

$$g(t) = g_P(t)\,\cos\omega_{RF}t + g_Q(t)\,\sin\omega_{RF}t \tag{2-14}$$

which implies that the total response of the impedance $Z(\omega)$ for the signal $f(t)$ in (2-6) consists of the in-phase response, modulated by $\cos\omega_{RF}t$, and the quadrature response, modulated by $\sin\omega_{RF}t$.

To prove (2-14), we only need to show that it is equivalent to,

$$G(\omega) = F(\omega)Z(\omega) \tag{2-15}$$

By using (2-12), (2-13), and (2-7), (2-9), the right hand side of (2-14) has the following Fourier form,

$$\begin{aligned} G(\omega) &= \frac{1}{2}\,(\,G_P(\omega+\omega_{RF}) + G_P(\omega-\omega_{RF})\,) + \frac{1}{2j}\,(\,G_Q(\omega+\omega_{RF}) - G_Q(\omega-\omega_{RF})\,) \\ &= \frac{1}{2}\,(\,F_L(\omega+\omega_{RF})Z_P(\omega+\omega_{RF}) + F_L(\omega-\omega_{RF})Z_P(\omega-\omega_{RF})\,) \\ &\quad + \frac{1}{2j}\,(\,F_L(\omega+\omega_{RF})Z_Q(\omega+\omega_{RF}) - F_L(\omega-\omega_{RF})Z_Q(\omega-\omega_{RF})\,) \end{aligned} \tag{2-16}$$

Substituting (2-10), (2-11) into (2-16), we have

$$G(\omega) = \frac{1}{2}\,(\,F_L(\omega+\omega_{RF})Z(\omega) + F_L(\omega-\omega_{RF})Z(\omega)\,) \tag{2-17}$$

Substituting (2-7), the equation (2-17) becomes (2-15). Therefore this part of the proof is completed.

When the beam passes the cavity gap, the in-phase response due to the cavity impedance, which is modulated by cos $\omega_{RF}t$, provides an almost constant force in the beam synchrotron oscillation, which will not affect the synchrotron oscillation directly. In fact this force will induce a synchronous phase shift and therefore the RF driving system can provide a compensation through the phase feedback. On the other hand, the quadrature response is modulated by sin $\omega_{RF}t$, which is in the same fashion as that of the RF driving wave and therefore functions as the same as that the RF driving wave does. In other words, this force generates a bucket in the phase space, which affects the synchrotron oscillation directly. Therefore, if the instability of the the synchrotron oscillation is concerned, the effect of the in-phase response can be neglected, and the quadrature response becomes a dominant factor. It follows,

$$Z_M(\omega) = Z_Q(\omega) \tag{2-18}$$

and therefore (2-5) is proved by substituting (2-11).

2.3. Impedance of RF cavity

In this subsection, we present the transfer function of the impedance of (2-5) for the RF cavity.

Consider an RF cavity with the resonant frequency ω_R, the shunt resistance R, and the half-bandwidth σ, which can be written as,

$$\sigma = \frac{\omega_R}{2Q} \tag{2-19}$$

where Q is the quality factor of the cavity. The transfer function of the cavity is,

$$Z(s) = \frac{2\sigma R s}{s^2 + 2\sigma s + \omega_R^2} \tag{2-20}$$

We assume that

$$\omega_{RF} \approx \omega_R \gg \omega \approx \omega_S \tag{2-21}$$

Let the cavity be detuned from ω_{RF} by an angle ϕ_Z. We have

$$\omega_{RF} - \omega_R \approx \sigma \tan\phi_Z \tag{2-22}$$

We write,

$$Z(s+j\omega_{RF}) = \frac{2\sigma Rs + 2j\sigma R\,\omega_{RF}}{s^2 + 2j\omega_{RF}s - \omega_{RF}^2 + 2\sigma s + 2j\sigma\omega_{RF} + \omega_R^2} \tag{2-23}$$

In the numerator, since $|s| = \omega << \omega_{RF}$, the term $2\sigma Rs$ can be neglected. In the denominator, since that if $Q >> 1$, $\sigma = \frac{\omega_R}{2Q} << \omega_{RF}$, then compared with either $2j\omega_{RF}s$ or $2j\sigma\omega_{RF}$, the term $2\sigma s$ can be neglected. Also, if $|\omega_R^2 - \omega_{RF}^2| >> |s^2| = \omega^2$, we have,

$$\omega_R^2 - \omega_{RF}^2 + s^2 \approx \omega_R^2 - \omega_{RF}^2 \tag{2-24}$$

Using

$$\omega_R^2 - \omega_{RF}^2 \approx -2\omega_{RF}(\omega_{RF} - \omega_R) = -2\omega_{RF}\sigma\tan\phi_Z \tag{2-25}$$

we get,

$$Z(s+j\omega_{RF}) \approx \frac{2j\sigma R\,\omega_{RF}}{2j\omega_{RF}s + 2j\sigma\omega_{RF} - 2\omega_{RF}\sigma\tan\phi_Z} = \frac{\sigma R}{s + \sigma + j\sigma\tan\phi_Z} \tag{2-26}$$

In a similar way we get,

$$Z(s-j\omega_{RF}) \approx \frac{\sigma R}{s + \sigma - j\sigma\tan\phi_Z} \tag{2-27}$$

Substituting (2-26) and (2-27) into (2-5), the longitudinal impedance of the RF cavity becomes,

$$Z_M(s) = \frac{-R\sigma^2\tan\phi_Z}{s^2 + 2\sigma s + \sigma^2(1 + \tan^2\phi_Z)} \tag{2-28}$$

4. Stability

To study the beam stability under the influence of the longitudinal impedance of RF cavity, we can write the following equation from Fig.1,

$$\phi = \frac{e\,\omega_O\,\omega_{RF}\,\eta V\cos\phi_S}{2\pi\beta^2 Es^2}\,\phi + \frac{e\,\omega_O\,\omega_{RF}\,\eta}{2\pi\beta^2 Es^2}\,Z_M(s)I_B\,\phi \tag{2-29}$$

Note that below transition,

$$\omega_S^2 = -\frac{e\,\omega_O\,\omega_{RF}\,\eta V\cos\phi_S}{2\pi\beta^2 E} \tag{2-30}$$

Substituting (2-30) into (2-29), we get,

$$s^2\phi + \omega_S^2\phi = \frac{\omega_S^2}{V\cos\phi_S} Z_M(s) I_B \ \phi \tag{2-31}$$

Define the ratio of the beam current to the generator current as [2,9],

$$Y = \frac{I_B}{I_{G0}} = \frac{I_B}{V/R} \tag{2-32}$$

where I_{G0} is the generator current without beam loading effect. Substituting (2-28), (2-32) and omitting the variable ϕ, the characteristic equation of the equation (2-31) becomes,

$$s^2 + \omega_S^2 = \frac{\omega_S^2 Y \sigma^2 \tan\phi_Z / \cos\phi_S}{s^2 + 2\sigma s + \sigma^2(1 + \tan^2\phi_Z)} \tag{2-33}$$

which is a fourth order dynamic system. Using Routh-Hurwitz table, it is straightforward to find the following stability conditions [9,12],

$$\tan\phi_Z > 0 \tag{2-34}$$

and

$$Y \tan\phi_Z \cos^2\phi_Z < \cos\phi_S \tag{2-35}$$

which are called the first and second Robinson criteria, respectively. The first criterion concerns just the detuning angle, and the second criterion concerns also the beam intensity, which is represented by Y.

III. Robinson and Pedersen Approach

The stability problem for bunched beam longitudinal dipole motion was first solved by Robinson [12], where the effect of the fundamental component of the beam phase deviation on the cavity phase deviation is considered to give rise to the stability criteria (2-34) and (2-35). Among later works, the Pedersen formulation [5,9] is of particular interest because where the phase and amplitude modulations and their cross effects due to the detuned cavity are treated separately, therefore the phase feedback and tuning control can be included in the dynamic model of the beam loading. The stability analysis gives rise to the same results as by Robinson.

In this section, we present the Pedersen formulation, and then it will be compared with the model presented in the last section.

3.1. Pedersen Formulation

In the Robinson and Pedersen approach of longitudinal bunched beam stability analysis, the perturbation source is the beam phase deviation. The stability is studied by finding the equivalent RF cavity phase deviation due to the beam phase deviation. The block diagram can be shown in Fig.2, where an inspection indicates that the upper loop is nothing more than a rearrangement of the synchrotron oscillation loop in Fig.1, and the transfer function $Z_{pp}^{T}(s)$ represents the total effect of the cavity voltage phase variation due to the beam phase deviation $\Delta\phi_B$.

To find the transfer function $Z_{pp}^{T}(s)$, several steps have to be followed. Since only the fundamental beam frequency at ω_{RF} is considered, the vector diagram shown in Fig.3 can be used, where I_G, I_B, and I_T are the generator, beam image, and the total currents, respectively. If the cavity detuning angle ϕ_Z is chosen properly as shown, which can be achieved by a tuning loop, then the total cavity voltage V_T can be kept unchanged under the beam loading.

The Pedersen approach considers the total effect on the phase variation of the cavity voltage V_T due to the variation of the phase of the beam current.

Step 1: Projection of I_B on I_T.

From Fig.3, we can write,

$$I_G - jI_B e^{-j\phi_S} = I_T e^{-j\phi_Z} \tag{3-1}$$

The relation of both phase and amplitude variation on I_B and I_T is,

$$I_G - j(I_B+\Delta I_B)e^{-j(\phi_S+\Delta\phi_B)} = (I_T+\Delta I_T)e^{-j(\phi_Z+\Delta\phi_T)} \tag{3-2}$$

By linearizing (3-2), subtracting (3-1) from (3-2), and equating the real and imaginary parts separately, we have,

$$\begin{bmatrix} \Delta I_T \\ I_T\Delta\phi_T \end{bmatrix} = \begin{bmatrix} \sin(\phi_Z-\phi_S) & -\cos(\phi_Z-\phi_S) \\ \cos(\phi_Z-\phi_S) & \sin(\phi_Z-\phi_S) \end{bmatrix} \begin{bmatrix} \Delta I_B \\ I_B\Delta\phi_B \end{bmatrix} \tag{3-3}$$

Step 2: Projection of I_T on V_T.

Under detuning, the impedance of the cavity can be written,

$$Z = R\cos\phi_Z e^{j\phi_Z} \tag{3-4}$$

Thus, we have

$$V_T = I_T e^{-j\phi_Z} Z = I_T R\cos\phi_Z \tag{3-5}$$

To find the static projection of I_T on V_T, we write,

$$(I_T + \Delta I_T)e^{-j\Delta\phi_T} R\cos\phi_Z = (V_T + \Delta V_T)e^{-j\Delta\phi_V} \tag{3-6}$$

Therefore, we get,

$$\begin{bmatrix} \Delta V_T \\ V_T\Delta\phi_V \end{bmatrix} = R\cos\phi_Z \begin{bmatrix} \Delta I_T \\ I_T\Delta\phi_T \end{bmatrix} \tag{3-7}$$

Since the bandwidth of the RF cavity is narrow, the transient response must be considered. The complete projection from I_T to V_T therefore is,

$$\begin{bmatrix} \Delta V_T \\ V_T\Delta\phi_V \end{bmatrix} = R\cos\phi_Z \begin{bmatrix} Z_{aa}(s) & Z_{pa}(s) \\ Z_{ap}(s) & Z_{pp}(s) \end{bmatrix} \begin{bmatrix} \Delta I_T \\ I_T\Delta\phi_T \end{bmatrix} \tag{3-8}$$

where $Z_{aa}(s)$ is the normalized transfer function from the amplitude variation of I_T to the amplitude variation of V_T, and so on for other transfer functions. These transfer functions are as follows [7,9],

$$Z_{aa}(s) = Z_{pp}(s) = \frac{1}{2}\left(\frac{Z(s+j\omega_{RF})}{Z(j\omega_{RF})} + \frac{Z(s-j\omega_{RF})}{Z(-j\omega_{RF})}\right) \tag{3-9}$$

and,

$$Z_{pa}(s) = -Z_{ap}(s) = \frac{1}{2j}\left(\frac{Z(s+j\omega_{RF})}{Z(j\omega_{RF})} - \frac{Z(s-j\omega_{RF})}{Z(-j\omega_{RF})}\right) \tag{3-10}$$

Using (2-26) and (2-27), we have,

$$Z(\pm j\omega_{RF}) = \frac{R}{1 \pm j\tan\phi_Z} \tag{3-11}$$

Substituting (2-26), (2-27), and (3-11) into (3-9) and (3-10), we get,

$$Z_{aa}(s) = Z_{pp}(s) = \frac{\sigma s + \sigma^2(1+\tan^2\phi_Z)}{s^2 + 2\sigma s + \sigma^2(1+\tan^2\phi_Z)} \tag{3-12}$$

and,

$$Z_{pa}(s) = -Z_{ap}(s) = \frac{-\sigma \tan\phi_Z s}{s^2 + 2\sigma s + \sigma^2(1+\tan^2\phi_Z)} \tag{3-13}$$

Step 3: Projection of beam phase variation $\Delta\phi_B$ to V_T.

Assuming $\Delta I_B = 0$, using (3-3) and (3-8), the total voltage phase variation due to the beam phase variation can be written as,

$$\Delta\phi_V = Z^B_{pp}(s)\Delta\phi_B = \frac{R}{V}\cos\phi_Z \begin{bmatrix} Z_{ap}(s) & Z_{pp}(s) \end{bmatrix} \begin{bmatrix} -I_B\cos(\phi_Z - \phi_S) \\ I_B\sin(\phi_Z - \phi_S) \end{bmatrix} \Delta\phi_B \tag{3-14}$$

Substituting (3-12) and (3-13) into (3-14), we get,

$$\begin{aligned} Z^B_{pp}(s) &= \frac{I_B}{V/R} \frac{-\sin\phi_S \sigma s + \sigma^2\cos\phi_Z \sin(\phi_Z - \phi_S)(1+\tan^2\phi_Z)}{s^2 + 2\sigma s + \sigma^2(1+\tan^2\phi_Z)} \\ &= Y \frac{-\sin\phi_S \sigma s + \sigma^2(\tan\phi_Z \cos\phi_S - \sin\phi_S)}{s^2 + 2\sigma s + \sigma^2(1+\tan^2\phi_Z)} \end{aligned} \tag{3-15}$$

Also from,

$$\Delta V_T = Z^B_{pa}(s)\Delta\phi_B = R\cos\phi_Z \begin{bmatrix} Z_{aa}(s) & Z_{pa}(s) \end{bmatrix} \begin{bmatrix} -I_B\cos(\phi_Z - \phi_S) \\ I_B\sin(\phi_Z - \phi_S) \end{bmatrix} \Delta\phi_B \tag{3-16}$$

we have,

$$\begin{aligned} Z^B_{pa}(s) &= RI_B \frac{-\cos\phi_S \sigma s - \sigma^2\cos\phi_Z \cos(\phi_Z - \phi_S)(1+\tan^2\phi_Z)}{s^2 + 2\sigma s + \sigma^2(1+\tan^2\phi_Z)} \\ &= RI_B \frac{-\cos\phi_S \sigma s - \sigma^2(\tan\phi_Z \sin\phi_S + \cos\phi_S)}{s^2 + 2\sigma s + \sigma^2(1+\tan^2\phi_Z)} \end{aligned} \tag{3-17}$$

Step 4: Total equivalent projection of $\Delta\phi_B$ on $\Delta\phi_V$.

In order to develop the total projection of $\Delta\phi_B$ on $\Delta\phi_V$, including the contribution of voltage amplitude variation ΔV, the equivalent phase deviation of the RF voltage due to ΔV is needed. Note that the total particle energy gain due to the RF voltage amplitude and phase variation is proportional to

$$(V + \Delta V)\sin(\phi_S + \Delta\phi_V) - V\sin\phi_S \approx (V + \Delta V)\cos\phi_S \Delta\phi_V + \Delta V \sin\phi_S \tag{3-18}$$

Letting $\Delta V = 0$ and $\Delta\phi_V = 0$, separately, and equating each gain leads to

$$\Delta\phi_V = \frac{\tan\phi_S}{V}\,\Delta V \tag{3-19}$$

Therefore consider the contribution of $Z^B_{pa}(s)$, the total transfer function from $\Delta\phi_B$ to $\Delta\phi_V$ is,

$$Z^T_{pp}(s) = Z^B_{pp}(s) + \frac{\tan\phi_S}{V}\,Z^B_{pa}(s) = \frac{Y\sigma^2\tan\phi_Z/\cos\phi_S}{s^2 + 2\sigma s + \sigma^2(1+\tan^2\phi_Z)} \tag{3-20}$$

3.2. Stability

From Fig.2, we have

$$\phi = \frac{e\,\omega_O\,\omega_{RF}\,\eta V\cos\phi_S}{2\pi\beta^2 E s^2}\,\phi - \frac{e\,\omega_O\,\omega_{RF}\,\eta V\cos\phi_S}{2\pi\beta^2 E s^2}\,Z^T_{pp}(s)\,\phi \tag{3-21}$$

Using (2-30), the equation (3-21) can be written as,

$$s^2\phi + \omega_S^2\phi = \omega_S^2 Z^T_{pp}(s)\,\phi \tag{3-22}$$

Substituting (3-20) into (3-22), and leaving off ϕ, we get the same characteristic equation of that of (2-33). This shows that the two approaches are equivalent with respect to the dipole motion instability.

3.3. Comparison

In deriving the transfer function $Z_M(s)$ in Fig.1, the in-phase and quadrature transfer functions $Z_P(s)$ and $Z_Q(s)$ are used. To determine the beam stability under beam loading, it it shown that the quadrature transfer function plays a key role. In deriving the transfer function $Z^T_{pp}(s)$ in Fig.2, the phase to phase, amplitude to amplitude, and the phase to amplitude, amplitude to phase transfer functions, $Z_{pp}(s)$, $Z_{aa}(s)$, and $Z_{pa}(s)$, $Z_{ap}(s)$, respectively, are used. The total equivalent transmission from the beam phase variation to the induced cavity voltage phase deviation, i.e., $Z^T_{pp}(s)$, determines the system stability.

In Fig.4, the step responses of these transfer functions are shown, where the parameters of the AGS upgraded RF cavity are used, and the detuned angle ϕ_Z is at 40 degrees. From these responses, the fundamental difference between the two types of the transfer functions, and the two approaches as well, can be observed.

IV. Sacherer Integral Equation

In this section, we present the solution of the dipole coherent motion solved by using the Sacherer integral equation.

4.1. Sacherer integral equation for dipole motion

Consider the Vlasov equation,

$$\frac{\partial \psi}{\partial t} + \dot{\phi}\frac{\partial \psi}{\partial \phi} + \ddot{\phi}\frac{\partial \psi}{\partial \dot{\phi}} = 0 \tag{4-1}$$

where $\psi\,(\phi,\dot{\phi},t)$ is the normalized phase space density, and ϕ is the particle phase deviation. Using the phase space co-ordinates $(\phi,\dot{\phi}/\omega_S)$, and the polar phase space co-ordinates,

$$\phi = r\cos\theta \tag{4-2}$$

$$\dot{\phi}/\omega_S = r\sin\theta \tag{4-3}$$

the equation (4-1) can be written as,

$$\frac{\partial \psi}{\partial t} - \omega_S\frac{\partial \psi}{\partial \theta} + (\ddot{\phi} + \omega_S^2\phi)\frac{\partial \psi}{\partial \dot{\phi}} = 0 \tag{4-4}$$

The phase space density can be seen as a large time independent part ψ_0 and a small perturbation part ψ_1, which oscillates with frequency ω,

$$\psi\,(r,\theta,t) = \psi_0(r,\theta) + \psi_1(r,\theta)e^{j\omega t} \tag{4-5}$$

We note that in (4-4), the term $\ddot{\phi} + \omega_S^2\phi$ represents a first order quantity, therefore $\dfrac{\partial \psi}{\partial \dot{\phi}}$ can be replaced by

$$\frac{\partial \psi_0}{\partial \dot{\phi}} = \frac{\sin\theta}{\omega_S}\,\frac{d\psi_0}{dr} \tag{4-6}$$

The linearized Vlasov equation therefore is,

$$j\omega\psi_1 e^{j\omega t} - \omega_S\frac{\partial \psi_1}{\partial \theta}e^{j\omega t} + (\ddot{\phi} + \omega_S^2\phi)\,\frac{\sin\theta}{\omega_S}\,\frac{d\psi_0}{dr} = 0 \tag{4-7}$$

In the next, we discuss the coherent electromagnetic force represented by $\ddot{\phi} + \omega_S^2\phi$. Similarly to (2-31), in a time domain version, we can write,

$$\ddot{\phi} + \omega_S^2\phi = -\frac{\omega_S^2}{V\cos\phi_S}\,V_1(\phi) \tag{4-8}$$

where $V_1(\phi)$ represents the cavity voltage induced by the perturbation term $\psi_1(r,\theta)e^{j\omega t}$ in (4-5). To determine $V_1(\phi)$, we define the line density $\lambda(\phi)$, which is the projection of $\psi_1(r,\theta)$ on the ϕ - axis,

$$\lambda(\phi) = \int_{-\infty}^{\infty} \psi_1(\phi,\dot{\phi}/\omega_S)\, d\dot{\phi}/\omega_S \tag{4-9}$$

The line density can be Fourier expanded as,

$$\lambda(\phi) = \frac{1}{2\pi} \sum_{p=-\infty}^{\infty} \Lambda(p) e^{jp\phi} \tag{4-10}$$

where

$$\Lambda(p) = \int_{-\infty}^{\infty} \lambda(\phi) e^{-jp\phi}\, d\phi \tag{4-11}$$

Using (4-10), we obtain,

$$V_1(\phi) = -I_0 e^{j\omega t} \sum_{p=-\infty}^{\infty} Z(p)\Lambda(p) e^{jp\phi} \tag{4-12}$$

where $Z(p)$ is the corresponding impedance. Substituting (4-12) into (4-8), we get,

$$\ddot{\phi} + \omega_S^2 \phi = -\frac{\omega_S^2 I_0}{V\cos\phi_S} e^{j\omega t} \sum_{p=-\infty}^{\infty} Z(p)\Lambda(p) e^{jp\phi} \tag{4-13}$$

We emphasize that $V_1(\phi)$ is the voltage generated by the line density $\lambda(\phi)$ in (4-9), which applies only to the particles with the phase position ϕ. Therefore the equation (4-13) is not a regular synchrotron oscillation equation, such as (2-31), and to solve it for the synchrotron motion is not justifiable.

For dipole motion only, the perturbation distribution can be written,

$$\psi_1(r,\theta) = R_1(r) e^{j\theta} \tag{4-14}$$

where $R_1(r)$ is the radial function of dipole motion. Substituting (4-13), (4-14) into (4-7), and leaving off $e^{j\omega t}$, we get,

$$j(\omega - \omega_S) R_1(r) e^{j\theta} = \frac{\omega_S I_0}{V\cos\phi_S} \sin\theta \frac{d\psi_0}{dr} \sum_{p=-\infty}^{\infty} Z(p)\Lambda(p) e^{jp\phi} \tag{4-15}$$

Multiplying both sides of (4-15) by $e^{-j\theta}$, and integrating over θ from 0 to 2π, we get,

$$(\omega - \omega_S) R_1(r) = \frac{-\omega_S I_0}{V\cos\phi_S} \frac{d\psi_0}{dr} \frac{1}{r} \sum_{p=-\infty}^{\infty} \frac{Z(p)}{p} J_1(pr)\Lambda(p) \tag{4-16}$$

where we have used (4-2) and the integral

$$\int_0^{2\pi} e^{j(pr\cos\theta - m\theta)}\sin\theta \; d\theta = -\frac{2\pi m}{pr} j^m J_m(pr) \tag{4-17}$$

with $m=1$.

The equation (4-16) is the Sacherer integral equation for dipole motion [3,13,17].

4.2. Stability

To determine the beam stability, the Fourier coefficient $\Lambda(p)$ in (4-16) is needed. Using (4-11), (4-9), (4-14), and the relation,

$$d\phi \; d\dot{\phi}/\omega_S = r dr d\theta \tag{4-18}$$

we have,

$$\Lambda(p) = \int_{-\infty}^{\infty} \lambda(\phi) e^{-jp\phi} \; d\phi = \int_{-\infty}^{\infty} (\int_{-\infty}^{\infty} \psi_1(\phi, \dot{\phi}/\omega_S) \; d\dot{\phi}/\omega_S) e^{-jp\phi} \; d\phi$$

$$= \int_0^{\infty} r R_1(r) \; dr \int_0^{2\pi} e^{-j(\theta - pr\cos\theta)} \; d\theta = \frac{2\pi}{j} \int_0^{\infty} R_1(r) J_1(pr) r dr \tag{4-19}$$

Substituting (4-19) into (4-16), multiplying both sides of (4-16) by $2\omega_S r J_1(r)$, integrating over r [6,14], and picking up $p = \pm 1$, we get,

$$2\omega_S(\omega - \omega_S) = \frac{-4\pi\omega_S^2 I_0}{V\cos\phi_S} (\int_0^{\infty} J_1^2(r) \frac{d\psi_0}{dr} \; dr) \; \frac{1}{j} \; (\; Z(\omega + \omega_{RF}) - Z(\omega - \omega_{RF}) \;) \tag{4-20}$$

where we used

$$J_1(-r) = -J_1(r) \tag{4-21}$$

Using

$$2\omega_S(\omega - \omega_S) \approx \omega^2 - \omega_S^2 \tag{4-22}$$

the equation (4-20) becomes,

$$\omega^2 - \omega_S^2 = \frac{4\pi\omega_S^2 I_0}{V\cos\phi_S} (\int_0^{\infty} J_1^2(r) \frac{d\psi_0}{dr} \; dr) \; \frac{1}{j} \; (\; Z(\omega + \omega_{RF}) - Z(\omega - \omega_{RF}) \;) \tag{4-23}$$

Substituting $s = j\omega$, and using (2-5), (2-28), it can be written as,

$$s^2 + \omega_S^2 = \frac{8\pi\omega_S^2 I_0}{V\cos\phi_S} (\int_0^{\infty} J_1^2(r) \frac{d\psi_0}{dr} \; dr) \; Z_M(s) \tag{4-24}$$

which is equivalent to (2-31) and (2-33) except for a scaling difference. Note that for delta functions, we have $I_B = 2I_0$. To solve the integral in (4-24), a specific static distribution is needed.

V. Generalize the Formulation

In Section II, the impedance $Z_M(s)$ is derived under the consideration of the synchrotron oscillation modulated by the RF frequency. In a real situation of rigid bunch motion, the beam current signal contains other frequency components, and also the signal scaling has to be considered. Therefore to generalize the formulation to the rigid bunch motion, the beam current signal needs to be analyzed. For each component in the signal, the effective impedance can be found, which needs only a trivial modification from the results in Section II. The summation of the effects of the impedance due to each component in the signal is the force the beam received. In the treatment, a form factor will emerge.

5.1. Signal of rigid bunch motion

Let T_{RF} be the RF period, i.e.,

$$T_{RF} = \frac{2\pi}{h\,\omega_0} = \frac{2\pi}{\omega_{RF}} \tag{5-1}$$

A beam longitudinal signal with N particles in a bunch can be written as,

$$i(t) = Ne \sum_{k=-\infty}^{\infty} \delta\left(t - kT_{RF} + \tau \cos\omega_S kT_{RF}\right) \tag{5-2}$$

where τ is the synchrotron oscillation amplitude in time.

The spectrum of this signal can be calculated as [16],

$$\begin{aligned} I(\omega) &= Ne \int_{-\infty}^{\infty} \sum_{k=-\infty}^{\infty} \delta\left(t - kT_{RF} + \tau \cos\omega_S kT_{RF}\right) e^{-j\omega t}\, dt \\ &= Ne \sum_{k=-\infty}^{\infty} e^{-j\omega(kT_{RF} - \tau \cos\omega_S kT_{RF})} = Ne \sum_{k=-\infty}^{\infty} e^{-j\omega kT_{RF}} \sum_{m=-\infty}^{\infty} j^m J_m(\omega\tau) e^{jm\omega_S kT_{RF}} \\ &= Ne\,\omega_{RF} \sum_{p=-\infty}^{\infty} \sum_{m=-\infty}^{\infty} j^m J_m(\omega\tau)\, \delta\left(\omega - p\,\omega_{RF} - m\,\omega_S\right) \end{aligned} \tag{5-3}$$

where the identities

$$e^{j\omega\tau\cos\omega_S kT_0} = \sum_{m=-\infty}^{\infty} j^m J_m(\omega\tau) e^{jm\omega_S kT_0} \tag{5-4}$$

and

$$\sum_{k=-\infty}^{\infty} e^{-j\Omega kT_{RF}} = \sum_{p=-\infty}^{\infty} \omega_{RF}\ \delta(\Omega - p\,\omega_{RF}) \tag{5-5}$$

are used.

We further assume that the bunches have a Gaussian distribution with an effective bunch length τ_L. The reason to choose the Gaussian distribution is for convenience. For each bunch, we have the following line density,

$$i_0(t) = \frac{2}{\tau_L}\left(\frac{2}{\pi}\right)^{1/2} e^{-8t^2/\tau_L^2} \tag{5-6}$$

With the average beam current

$$I_0 = \frac{Ne\,\omega_{RF}}{2\pi} \tag{5-7}$$

and using the phase oscillation amplitude

$$r = \omega_{RF}\tau \tag{5-8}$$

the equation (5-3) becomes [16],

$$I(\omega) = 2\pi I_0 \sum_{p=-\infty}^{\infty} \sum_{m=-\infty}^{\infty} j^m J_m(r\,\omega/\omega_{RF}) e^{-(r_L\omega/\omega_{RF})^2/32}\ \delta(\omega - p\,\omega_{RF} - m\,\omega_S) \tag{5-9}$$

which is the spectrum of the rigid bunch motion.

5.2. Generalization

To compare the spectrum of the rigid bunch motion (5-9) with the signal used to develop the formulation in Section II, we let an idealized RF frequency modulated synchrotron oscillation signal to be,

$$i_1(t) = I_B r\ \cos\omega_S t\ \sin\omega_{RF} t \tag{5-10}$$

whose spectrum can be written as,

$$I_1(\omega) = 2\pi I_B r\ \frac{1}{4j} \sum_{p=\pm1} \sum_{m=\pm1} (-p)\ \delta(\omega - p\,\omega_{RF} - m\,\omega_S) \tag{5-11}$$

The first difference between the real rigid bunch motion signal represented by (5-9) and the idealized signal (5-11) is that (5-9) contains not only RF frequency modulation but also RF harmonics modulation, i.e., by the frequencies $p\,\omega_{RF}$, $|p|>1$. To justify the corresponding effective longitudinal impedance for these components, it is convenient to take the beam signal as approximately a delta function series, then to consider its frequency decomposition, such as,

$$\sum_{k=-\infty}^{\infty} \delta(t - kT_{RF}) = \frac{1}{T_{RF}} \sum_{p=-\infty}^{\infty} e^{jp\,\omega_{RF}\,t} = \frac{1}{T_{RF}} \left(1 + 2 \sum_{p=1}^{\infty} \cos p\,\omega_{RF}\,t \right) \qquad (5\text{-}12)$$

Note that all the frequency components are in cosine waveform. Furthermore, at the bunch passing time $t = kT_{RF}$, these components become $\cos p\,2\pi k$, $p = 0, 1, \cdots$, which shows that in the decomposition, at the beam passage these cosine functions have no phase shift for all p. Therefore concerning the effective longitudinal impedance the same argument as that in Section II can be used for $p \neq 1$, and the conclusion is that the quadrature responses still determine the effective longitudinal impedance for all p. Thus we have $Z_M(\omega) = Z_Q(\omega)$ not only for the RF frequency modulation, but also for the RF harmonic modulation. For the carrier component with the frequency $p\,\omega_{RF}$, the variable ω_{RF} in (2-11) should however be replaced by $p\,\omega_{RF}$. In the system synthesis, firstly these frequency components in the rigid bunch motion signal should be identified, then the corresponding longitudinal impedances should be used to find the induced forces. The combined force is the one the beam received.

The second difference of (5-9) from (5-11) is that it contains not only dipole motion but also high mode motion, i.e., $m\,\omega_S$, $|m|>1$. If only the dipole motion is concerned, this aspect can be overlooked.

The third difference is that in (5-9), the spectrum amplitude is affected by several factors, such as the Bessel function, the bunch distribution and the bunch length. The combined influence of these factors can be called a form factor, which should be multiplied to the scaling I_B in Fig.1. If the synchrotron oscillation frequency is assumed to be constant, then this modification will change the stability margin. A detailed discussion will be presented in the following.

5.3. Form factor

Consider the most important case of dipole motion with RF frequency modulation, where $p = \pm 1$ and $m = \pm 1$. We write (5-9) as,

$$I(\omega) = 2\pi I_0 \sum_{p=\pm 1} \sum_{m=\pm 1} j^m J_m(r\,\omega/\omega_{RF}) e^{-(r_L\,\omega/\omega_{RF})^2/32}\, \delta\,(\omega - p\,\omega_{RF} - m\,\omega_S) \tag{5-13}$$

Since $J_m(r\,\omega/\omega_{RF})$ is evaluated at $\omega = \pm\omega_{RF} \pm \omega_S \approx \pm\omega_{RF}$, and we have,

$$J_1(-x) = -\,J_1(x) \tag{5-14}$$

$$J_{-1}(x) = -\,J_1(x) \tag{5-15}$$

the equation (5-13) can be written as,

$$I(\omega) = 8\pi I_0 J_1(r\,|\omega|/\omega_{RF}) e^{-(r_L\,\omega/\omega_{RF})^2/32} \frac{1}{4j} \sum_{p=\pm 1} \sum_{m=\pm 1} (-p)\, \delta\,(\omega - p\,\omega_{RF} - m\,\omega_S) \tag{5-16}$$

Using the standard relation between the average beam current I_0 and the beam current at the fundamental frequency I_B, for the delta series distribution,

$$I_B = 2I_0 \tag{5-17}$$

the form factor can be written as,

$$F = \frac{I(\omega)}{I_1(\omega)} = \frac{2J_1(r\,|\omega|/\omega_{RF})}{r}\, e^{-(r_L\,\omega/\omega_{RF})^2/32} \approx \frac{2J_1(r)}{r}\, e^{-(r_L\,\omega/\omega_{RF})^2/32} \tag{5-18}$$

where in the simplification we consider that in this case $|\omega| \approx \omega_{RF}$.

The factor $\dfrac{2J_1(r)}{r}$ is plotted in Fig.5, which shows that if the phase oscillation amplitude varies within 1 *rad*, the error caused by using the idealized dipole motion model is not larger than 12 % compared to the rigid bunch dipole motion.

Consider the longitudinal dipole motion discussed in Section II again, where only the synchrotron oscillation modulated by RF frequency is concerned. The form factor F in (5-18) has to be multiplied to the scaling I_B in Fig.1, and therefore also to $Y = \dfrac{I_B}{V/R}$ in (2-33). Thus, the new ratio of the beam current to the generator current

$$\overline{Y} = FY \tag{5-19}$$

will replace Y in the stability equation (2-35). Since $F<1$, the stability margin due to the beam loading effect defined in (2-35) is extended.

VI. Coupled Bunch Instabilities

A typical coupled bunch motion is generated by the impedance of a resonator, such that the relative phase position of the adjacent bunches is changed in phase space in a certain mode for a period of the revolution, and therefore in the beam current signal a frequency shift can be observed. Several consequences of this change will be discussed by using the presented formulation.

6.1. Coupled bunch motion

Let there be h bunches, and let n be the coupled bunch mode number. There will be $n=0, 1, \ldots, h-1$ coupled bunch modes [4,13]. The phase difference between two adjacent bunches in the phase space is $\frac{2n\pi}{h}$. Since the period between the two adjacent bunches, i.e., the RF period, is $T_{RF}=\frac{2\pi}{h\omega_0}$, if one observes from a wall beam current monitor, frequency components of the coupled bunch mode $e^{j(n\omega_0+m\omega_S)t}$ will show up in the beam current signal. Corresponding to the longitudinal signal in (5-2), the signal of the coupled bunch motion can be written as,

$$i(t)=Ne\sum_{k=-\infty}^{\infty} e^{jn\omega_0 kT_{RF}}\,\delta(t-kT_{RF}+\tau\cos\omega_S kT_{RF}) \tag{6-1}$$

If further a rigid Gaussian distribution is also considered, then similar to (5-9), the spectrum of the signal observed from the wall monitor becomes,

$$I(\omega)=2\pi I_0\sum_{p=-\infty}^{\infty}\sum_{m=-\infty}^{\infty} j^m J_m(r\omega/\omega_{RF})e^{-(r_L\omega/\omega_{RF})^2/32}\,\delta(\omega-p\omega_{RF}-n\omega_0-m\omega_S) \tag{6-2}$$

where a frequency shift of the coupled bunch mode is shown.

If the coupled bunch instability is considered, then the coupled bunch mode $e^{jn\omega_0 t}$ can

be assumed to be a rigid wave, which is generated from the relative phase difference of the bunches in the phase space and then its induced force is applied back to these passing bunches. Thus for an individual bunch, which performs a synchrotron oscillation in the phase space, the modulation effects of the beam current signal due to the coupled bunch mode is demodulated. By the same argument as in Section II, the quadrature response represents the effective longitudinal impedance. Consider the effect of the frequency shift, we therefore have the following longitudinal impedance for the signal with RF modulation,

$$Z_M(\omega) = \frac{1}{2j}\left(Z(\omega+n\,\omega_0+\omega_{RF}) - Z(\omega+n\,\omega_0-\omega_{RF}) \right) \tag{6-3}$$

6.2. Coupled bunch instabilities

Combine the longitudinal impedance (6-3) with the consideration of the signal analysis (6-2), several results of coupled bunch instabilities follow.

Taking an example that $h = 4$ and $n = 1$, the coupled bunch modes are shown in Fig.6, where the fundamental spectrum lines of $p = \pm 1$ are directly from (6-3), and others are from the signal generalization (6-2).

If $n \neq 0$, then the two spectrum lines of the same frequency modulation may be far apart, for instance the two lines of $p = 1$ and $p = -1$ in Fig.6, and therefore in general the treatment for the resonator type impedance under the RF modulation such as that in Section II cannot be applied, and the spectrum lines may have to be treated separately. Consider the dipole upper sideband at $Z(\omega+\omega_0+\omega_{RF})$, and let the real part of the impedance be $\overline{R}$. Using $s = j\omega \approx j\omega_S$, the stability equation (2-31) can be written as,

$$s^2 + \omega_S^2 = \frac{\omega_S^2 I_B}{V\cos\phi_S}\,\frac{1}{2j}\,Z(\omega+\omega_0+\omega_{RF}) \approx \frac{\omega_S^2 I_B}{2V\cos\phi_S}\,\frac{\overline{R}}{j} \approx \frac{-\,\omega_S I_B \overline{R}}{2V\cos\phi_S}\,s \tag{6-4}$$

which can be written as,

$$s^2 + \frac{\omega_S I_B \overline{R}}{2V\cos\phi_S}\,s + \omega_S^2 = 0 \tag{6-5}$$

Below transition $\cos\phi_S > 0$, therefore the upper sideband is stable because that the coefficient of

s is positive. It follows that the lower sideband at $Z(\omega+\omega_0-\omega_{RF})$, which has a negative sign in (6-3), is unstable, and the opposite above transition.

It is interesting to revisit the form factor derived in Section V. We rewrite it as,

$$F = \frac{2J_1(r\,|\omega|/\omega_{RF})}{r} e^{-(r_L\omega/\omega_{RF})^2/32} \tag{6-6}$$

The simplification of the form factor in (5-18) cannot be made in the case of the coupled bunch mode, since now $|\omega|$ is not close to ω_{RF} if $n \neq 0$. Now both variables have to be considered in the Bessel function. In general, the influence of the synchrotron phase oscillation amplitude cannot be overlooked, such as the simplification in (5-18). Taking the AGS Booster as an example, the form factors for different r are shown in Fig.7. At the RF frequency of 2.55 MHz as shown both in Fig.5 and Fig.7, the influence of the variation of r is not significant. For the higher frequency, which is often of interest in the coupled bunch instabilities, this influence shows up. For a small variation, for instance in Fig.7 a range of r between 0.01 to 0.2, the form factors are approximately the same. This fact has the following implications. Once a coupled bunch motion has started, the signal frequency shift by the coupled bunch mode frequency can excite reactions from the longitudinal impedance at these frequencies. For each bunch, the synchrotron oscillation may get chance to grow, and so does the phase oscillation amplitude r appeared in the form factor (6-6). This amplitude, on the other hand, is also the amplitude of the coupled bunch mode. The insignificant influence of the variation of r in the process, shows the reason why we can assume that the coupled bunch mode is a rigid wave, when we consider the instability problem.

3. Examples of the AGS Booster and the AGS

In a test, a coupled bunch instability has been excited in the AGS booster by tuning an unused RF cavity [1]. The coupled bunch motion was observed in a long front porch, with the revolution frequency of 850 KHz. The harmonic number of the booster is 3, and the RF frequency was 2.55 MHz. In the test, the coupled bunch instability of a dipole mode was observed at the first revolution line, i.e., at 850 KHz, which implies that $n = 2$. There are

2×10^{11} protons in a bunch, therefore we have $I_0 = 0.082$ A and $I_B = 0.164$ A. The synchrotron oscillation frequency was about 4.3 KHz, the synchronous phase angle $\phi_S = 0$, and the RF voltage amplitude $V = 30$ KV.

The RF cavity used to excite the coupled bunch motion has a quality factor 2.5 and a shunt resistance 3 KΩ, it was tuned at the the revolution frequency in the test. The impedance of the cavity and also the driving RF cavity is shown in Fig.8.

To estimate the coupled bunch instability, the equation (6-5) can be used. To estimate the resistance $\overline{R}$ which is crucial in this test, the form factor in (6-6) is used, where the Gaussian distribution is still used since the associated error is not significant. The bunch length can be measured, which is $\tau_L \approx 130$ nS. The final effective resistance $\overline{R}$ of the unused cavity is shown in Fig.8 by dotted line, which indicate that it is 60 db, i.e., 1 KΩ at the 850 KHz. The growth rate calculated using (6-5) is about 27.7 mS, which is close to the test result of 30 mS.

In an AGS operation, a coupled bunch instability was observed and analyzed [10], which appeared at the 1.77 GeV front porch, with RF frequency of 4.18 MHz. It is a dipole motion with a coupled bunch mode $n = 11$, and the AGS has an RF harmonic number $h = 12$. To locate the frequency of the coupled bunch mode exciting resonator, two tests were performed. The bunch lengthes are 46 nS and 70 nS, and the beam currents are 0.089 A and 0.457 A, respectively. The RF voltages are 260 KV and 184 KV, the synchrotron frequencies are 1.64 KHz and 1.38 KHz, respectively. The observed growth rates are 48 mS and 24 mS, respectively. The form factors according to (6-6) are plotted in Fig.9, where a moderate $r = 0.1r_L$ is used. To generate the observed growth rates, the required resistances in the longitudinal impedance are plotted in Fig.10, which shows that at approximately 17.6 MHz the required resistances are crossed, note that the closest unstable coupled bunch mode frequency is at 17.1 MHz, therefore Fig.10 shows a possible location of the exciting resonator for the coupled bunch instability. This result agrees to the one obtained by different approaches [10].

Acknowledgment

The authors would like to thank M. Blaskiewicz, E.C. Raka, and A.M. Sessler for helpful discussions.

References

[1] M. Blaskiewicz, J.M. Brennan, and A. Ratti, *'Impedance of Booster Band II Cavity and the Associated Instabilities,'* AGS Studies Report, No. 271, 1992.

[2] D. Boussard, *'Design of a Ring RF System,'* CERN 91-04, 1991.

[3] A.W. Chao, *'Coherent Instabilities of A Relativistic Bunched Beams,'* AIP Conference Proceedings, 105, pp.353-523, 1983.

[4] A. Hofmann, *'Single-Beam Collective Phenomena - Longitudinal,'* CERN 77-13, pp.139-174, 1977.

[5] S. Koscielniak, *'A General Theory of Beam Loading,'* TRIUMF Design Note, TRI-DN-89-K25, 1989.

[6] J.L. Laclare, *'Bunched Beam Coherent Instabilities,'* CERN 87-03, pp.264-326, 1987.

[7] B.P. Lathi, *'Signals, Systems, and Communication'* John Willey & Sons, New York, 1965.

[8] A. Paupolis, *'The Fourier Integral and Its Applications,'* New York, McGraw-Hill, 1962.

[9] F. Pedersen, *'Beam Loading Effects in the CERN PS Booster,'* IEEE Trans. Nuclear Science, Vol. NS-22, pp.1906-1909, 1975.

[10] E.C. Raka, Private communication.

[11] G.H. Rees, *'Another Look at Coherent Longitudinal Instability of Bunched Beams,'* Proc. First European Particle Accelerator Conf. 1988.

[12] K.W. Robinson, *'Stability of Beam in Radio-Frequency Systems,'* Cambridge Electron Accelerator, CEAL-1010, Cambridge, Mass. 1964.

[13] F. Sacherer, *'Bunch Lengthening and Microwave Instability,'* IEEE Trans. Nuclear Science, Vol. 24, pp.1393-1395, 1977.

[14] T.F. Wang, *'Bunched Beam Longitudinal Mode-Coupling and Robinson-Type Instabilities,'* Particle Accelerators, Vol. 34, pp.105-126, 1990.

[15] S.Y. Zhang and W.T. Weng, *'Analysis of Acceleration Loops of a Synchrotron,'* Nuclear Instru. & Meth. in Physics Research, Vol. A317, pp.405-412, 1992.

[16] S.Y. Zhang and W.T. Weng, *'Spectrum Analysis in Beam Diagnoses,'* AGS Tech. Notes, No.372, BNL, 1993.

[17] B. Zotter, *'Longitudinal Stability of BUnched Beams, I: Resonator Impedances,'* CERN SPS/81-18, 1981.

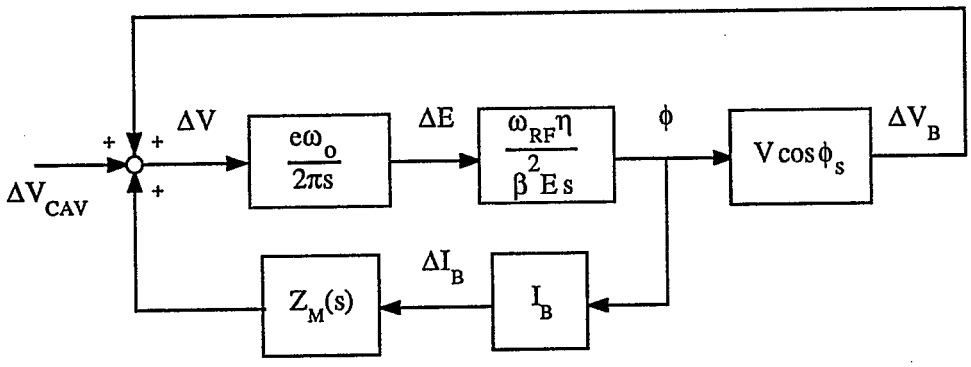

Fig.1. Beam Dynamic Model for Longitudinal Coherent Dipole Motion.

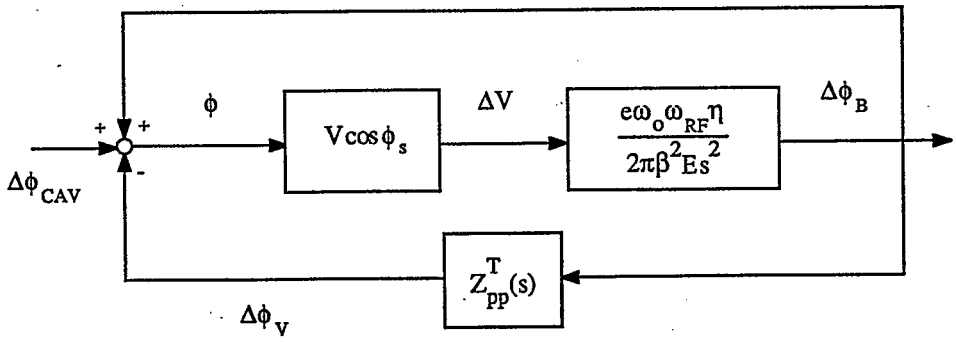

Fig.2. Beam Dynamic Model for Pedersen Formulation.

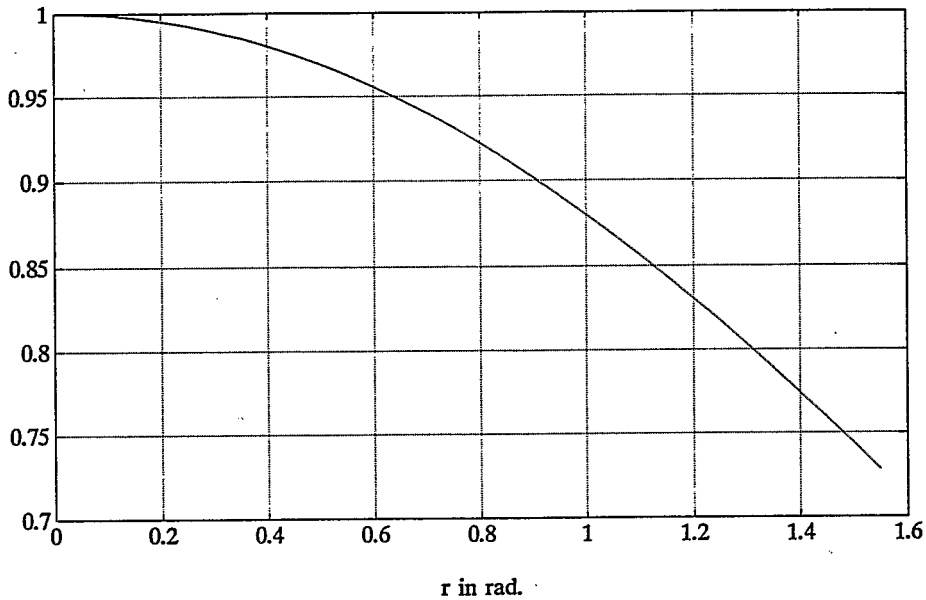

Fig.5. The Form Factor $2J_1(r)/r$.

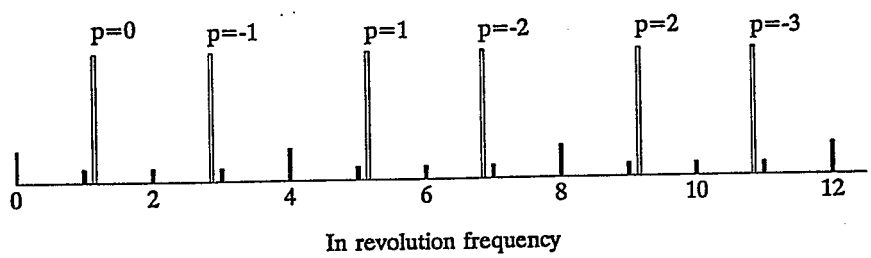

Fig.6. Coupled Bunch Spectrum Lines.

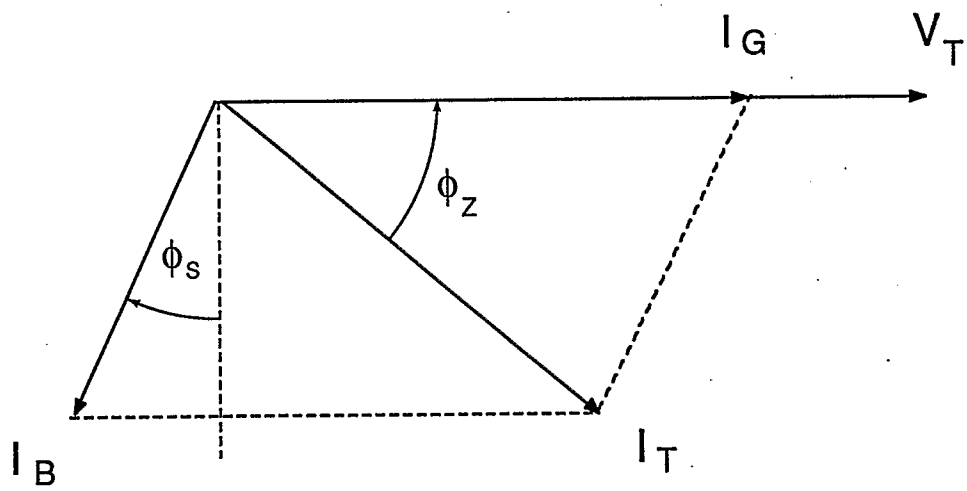

Fig.3. Vector Diagram of Beam Loading.

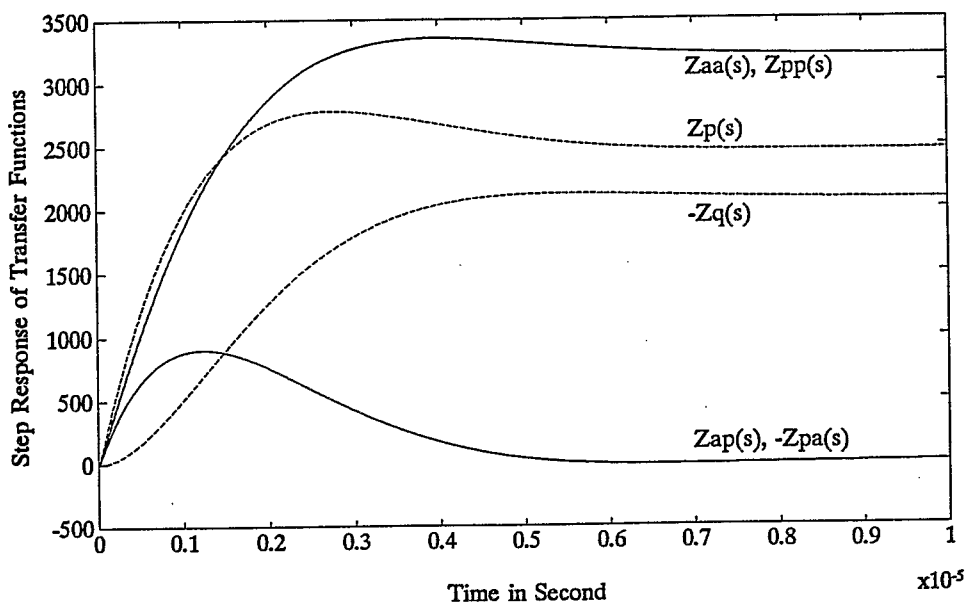

Fig.4. Step Responses for Different Transfer Functions.

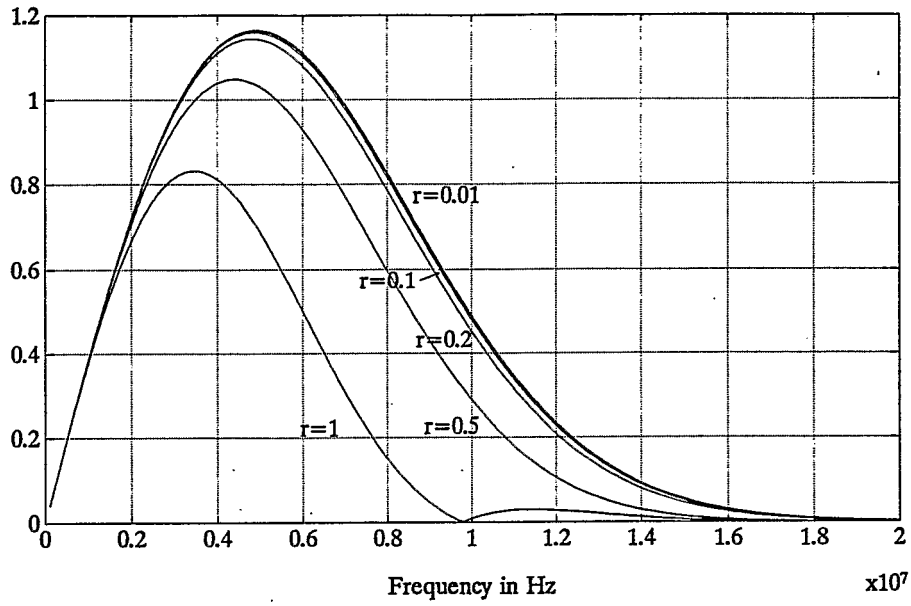

Fig.7. Form Factors with Different r.

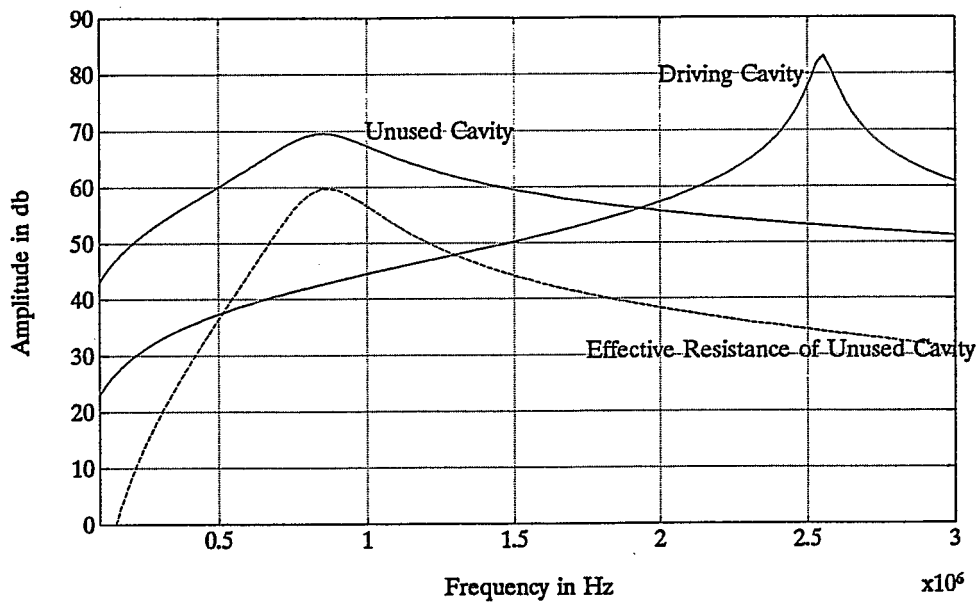

Fig.8. Impedance of the Driving RF Cavity and Unused Cavity in the AGS Booster.

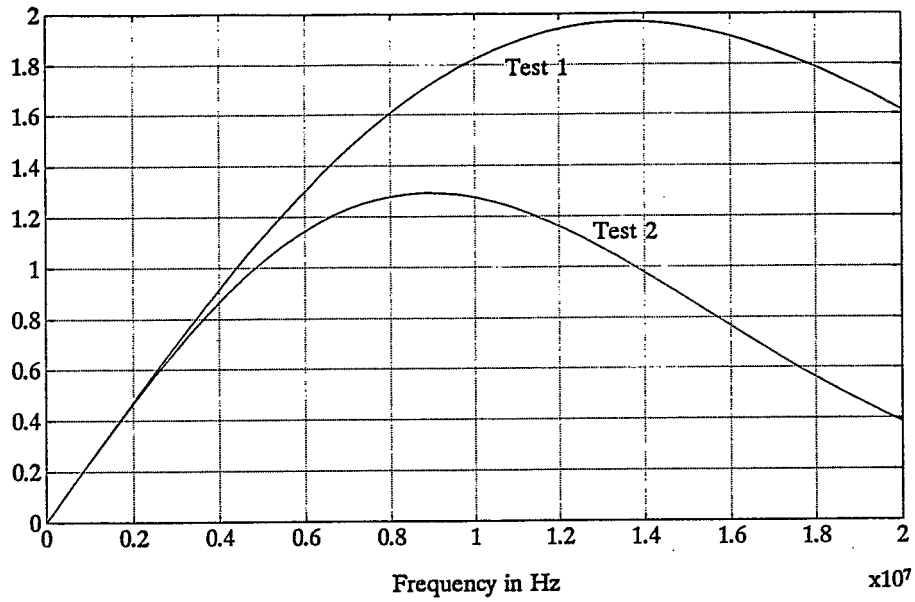

Fig.9. Form Factors of the Two Tests at AGS.

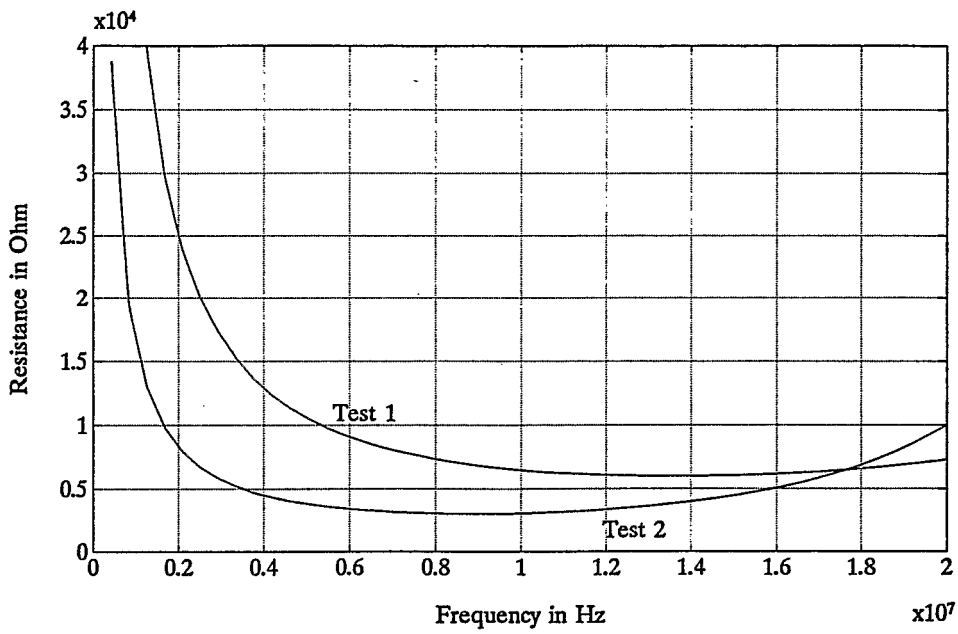

Fig.10. Resistances Required to Excite the Observed Growth Rates at AGS.